1Pb2-3

Real-time monitoring of viscosity in chemical reaction process by EMS system

Maiko Hosoda[1†], Yoshikazu Yamakawa[2], Keiji Sakai[3]
([1]Tokyo Denki University, [2]Triple-Eye Co. LTD., [3]Univ. of Tokyo)

1. Introduction

We can obtain various information on the state of materials through the viscosity measurement. Electro magnetically spinning (EMS) viscosity measurement system developed by us has an advantage that the rotational probe can be set in reaction and storage chambers since the driving torque is remotely conducted to the rotor from outside of the chamber. The driver applies a rotating magnetic field to the rotor made of electrically conductive materials. The interaction between the rotational magnetic field and the induced Lorentz current generates torque, which drives the probe so that it follows the rotation of the magnetic field. The magnitude of the driving torque is proportional to the deference in the rotational speeds of the magnetic field and the rotor, and the viscosity is determined as the ratio between the difference and the rotational speed of the probe rotor giving the shear deformation rate.

In our previous study, we proposed a new type of auto-standing probe, which is free from the coagulation from the sample liquid to the pivot of the rotor. The geometry of the rotor is modified so that the pivot is arranged at the top of the rotor in the air reservoir.

Some problems still remain to be solved. One is that the conventional geometry of the rotor and sample container is not suitable for the measurement in the chamber; the aspect ratio of the sample is quite high. For example, in the rotating plate type, the radius of the rotor is more than 10 times larger than the thickness of the sample. The situation is the same for the double cylinder type. We can not expect smooth and rapid exchange of the sample between the inside and outside of the measurement region. By assuming that the diffusion constant of molecules to be D=10^{-9} m^2/s, the diffusion of 10^{-2} m takes time of 10^5 s.

In this presentation, we propose a new devise that realize the smooth exchange of the sample fluid in the measurement region.

2. Viscometer with Permeable Substrate

The experimental configuration is shown in Fig.1. The rotor is a Yajirobe (auto-standing toy) type, which is supported at a pivot at the upper and central position of the rotor as shown in the figure. It automatically keeps its attitude perpendicular, and

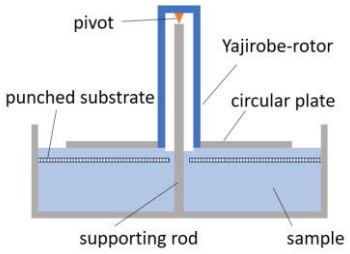

Fig.1 Schematic view of plate-plate type EMS viscometer with a permeable substrate.

the lower horizontal circular plate works as the rotor of the plate-plate type rotational viscometer. The feature of this rotor is that the pivot is not immersed in the sample, and we do not have to care the problem that the coagulation of the ingredients in the sample liquid might harm the smooth rotation of the viscosity probe.

In this experiment, the lower substrate is changed, which sandwiches thin liquid samples with the upper circular plate. Some kinds of plates are prepared; In the condition (a), a plane thin plate is employed as the substrate, which reproduces the generally used rotational viscometer. In (b), the substrate is removed, and the flow generated by the rotation of the upper circle plate diffuses downward. In this configuration, the region of the flow is known to extend to the order of the radius of the circle. In (c), (d), and (e), punched plates are employed as the lower substrate, which allows the transmission of the molecules through the thermal diffusion process. The holes are circle and arranged in the hexagonal symmetry. The geometry of the holes can be characterized by two parameters, the radius of the hole R, and the lattice constant L which is the distance between the nearest neighbors. The parameters are R =1.5 mm, L =4.0 mm for (c), R =1.0 mm, L=2.0 mm for (d) and R=0.5 mm, L =1.0 mm for (e). The occupation ratio of the holes against the surface area is 0.51 for (c) and 0.23 for (d) and (e).

The thickness of all the plates is 0.5 mm. For the above configuration, we measured the relation between the shear deformation rate and the applied torque, which are determined independently from the rotational speed of the rotor, and the difference between the rotational speeds of the magnetic fields and the probe rotor.

The sample used is the viscosity standard liquid

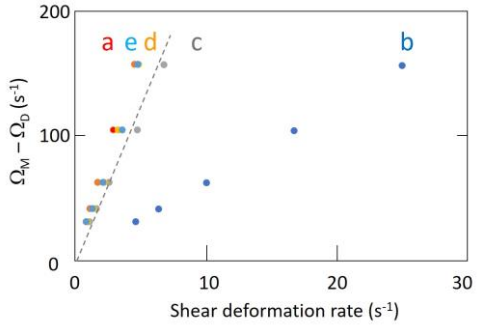

Fig.2 Relation between shear deformation rate and applied torque.

purchased from Shin-Etsu Chemical Co., Ltd., whose viscosity is 48.5 mPa·s at 25 °C. We employed this rather viscous sample so that the Reynolds's number remains below 10 and the effect of the inertia can be neglected.

The obtained results are shown in Fig.2. For all the substrates, the torque and the shar deformation rate shows the linear relation, which corroborates the punched plate can be employed for the substrate of the plate type viscometer.

As shown, remarkable difference is seen for curves of (a) and (b), which is quite reasonable since the required torque increases when the sample is confined in a thin space and the shear deformation rate determined by $\gamma = v/d$ decreases, where v is the speed of the upper plate and d is the sample thickness.

Next, we can see that the torque required for the substrate with punched structure (c)〜(e) decreases than that for the simple plane plate (a). It seems strange from the direct image, that the rugged substrate might disturb the smooth laminar flow of the sample, which would lead to the increase in the apparent viscosity. The observed behavior can be explained as follows; Note here, that the (kinetic) viscosity is the diffusion constant of the momentum. Let us consider the principle of the viscosity measurement with the plate-plate type viscometer from the viewpoint of the energy dissipation. The configuration of the following explanation is shown in Fig. 3. In the configuration of the plate-plate type viscometer (i), the moving upper plate gives the momentum with respect to lateral direction to the sample. It homogeneously diffuses downward and then retrieved by the lower plate. The shear deformation rate is homogeneous and $\gamma = v/d$ and the energy dissipation per unit volume due to the viscous process is $\eta\gamma^2$. For the surface area S, the energy injected per unit time is σSv, where σ is the stress applied to move the upper plate, while the whole energy dissipation is $\eta\gamma^2 dS$. These should be equal, and we obtain the following well known relation of,

$\sigma=\eta(v/d)$.

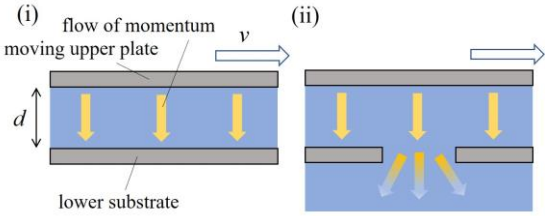

Fig.3 Diffusion of momentum in viscometer.

For the substrate having punched structure (ii), the momentum leaks out from the holes, which diffuses downward into the sample below the substrate. The volume concerning the momentum diffusion process increases, however, whole the dissipation decreases since that per unit volume is proportional to the square of the shear deformation rate.

Along the above story, we can roughly estimate the apparent viscosity as a function of R, L, p for each substrate. The detail would be given elsewhere, and we only give a result of calculation. The dashed line in Fig.2 is derived as the prediction for the substrate (c). which well reproduces the experimental result.

3. Conclusion

The most important knowledge obtain by the present experiment is that the punched substrate that allows the molecular exchange can be employed as the substrate of the rotational viscometer. The influence of the holes can be neglected when the diameter is as small as the sample thickness. For substrate with larger holes, the apparent torque decreases, which can be explained by considering the leakage of the momentum. The thickness of the sample liquid in the present experiment is 2 mm and the time required for the molecular diffusion is in the order of 10^3 s. The time resolution is satisfactorily high for the usual process of reaction and maturing.

In the presentation, we would show the result of the actual monitoring of the chemical and physical process.

References

1. M. Hosoda, T. Hirano, Y. Yamakawa and K. Sakai, Jpn. J. Appl. Phys. 58 SGGA01 1-4 (2019).
2. T. Hirano, S. Mitani and K. Sakai Jpn. J. Appl. Phys. 58 SGGA03 1-4 (2019).
3. T. Hirano, S. Mitani and K. Sakai Jpn. J. Appl. Phys. 59 SKKA01 1-4 (2020).
4. M. Hosoda, T. Hirano, Y. Yamakawa and K. Sakai, Jpn. J. Appl. Phys. 59 SKKA09 1-4 (2020).
5. M. Hosoda, Y. Yamakawa and K. Sakai Jpn. J. Appl. Phys. 60 SDDB04(2021).
6. K. Sakai, Jpn. J. Appl. Phys. 60 SD0801(2021).